Acta Geotechnica (2020) 15:1231–1241
https://doi.org/10.1007/s11440-019-00818-6

RESEARCH PAPER

Shakedown analysis of ballasted track structure using three-dimensional finite element techniques

Kangyu Wang[1] · Yan Zhuang[2,3] · George Kouretzis[4] · Scott William Sloan[4]

Received: 25 April 2018 / Accepted: 14 May 2019 / Published online: 28 May 2019

Abstract
Shakedown analysis is an attractive method for determining the capacity of geostructures to sustain repeated loads involving a large number of cycles, e.g. rolling and sliding train wheel loads. Its main advantage is that it comes at a significantly reduced computational cost, compared to standard time-domain analyses. An essential component of shakedown analysis is the derivation of closed-form solutions to compute stresses due to the external repeated loads, a task that is not always feasible for complex problems as the ballasted rail track discussed herein. To tackle this, we present in this paper the use of finite element tools to obtain a quasi-lower-bound shakedown load numerically. The proposed method is based on the computation of the three-dimensional elastic stress field numerically, and the estimation of the shakedown load iteratively via an optimisation subroutine implemented in ABAQUS. Following a short presentation of this concept, we compare the elastic stress fields from models featuring varying degree of complexity, with the aim of identifying an optimal discretisation of the problem. This approach can be used for optimising the design of ballasted track structure, and this concept is briefly presented via a parametric study.

Keywords Ballast track structure · Finite element method · Lower-bound shakedown theorem · Shakedown analysis

1 Introduction

Operation costs of railway lines increase due to track deterioration associated with cumulative irreversible (plastic) deformations of the ballasted track structure, which may result in rail bending or crack formation in the subgrade. Such modes of failure may compromise the riding comfort and the safety of moving trains [26, 32]. It is therefore important to determine the design load level, below which a given track structure will not experience accumulation of significant plastic strains leading to fatigue failure after a large number of load cycles, but rather plastic strains will reach a safe steady state. Current design codes for railways generally embrace empirical relations or solutions based on the theory of elasticity for the determination of design loads, which cannot take into account the complex nature of the load applied from a moving train or consider the elastoplastic nature of track structure materials.

Shakedown analysis, on the other hand, is a robust tool that allows modelling phenomena such as instantaneous collapse, fatigue and accumulation of excessive plastic

✉ Yan Zhuang
zhuangyan4444@hotmail.com

Kangyu Wang
kangyuwang@zjut.edu.cn

George Kouretzis
georgios.kouretzis@newcastle.edu.au

Scott William Sloan
scott.sloan@newcastle.edu.au

[1] School of Civil Engineering and Architecture, Zhejiang University of Technology, Hangzhou 310014, China

[2] Key Laboratory for RC and PRC Structures of Education Ministry, School of Civil Engineering, Southeast University, No. 2 Sipailou, Nanjing 210096, Jiangsu, China

[3] National Engineering Laboratory of Highway Maintenance Technology, Changsha University of Science and Technology, Changsha 410114, Hunan, China

[4] ARC Centre of Excellence for Geotechnical Science and Engineering, Faculty of Engineering and Built Environment, The University of Newcastle, Callaghan, NSW 2308, Australia

strains in structure subjected to cyclic loading. The shakedown limit load has been used since the 1960s for the rational design of metallic contacts such as rails, roller bearings, and traction drives [12]. This limit load can be calculated by means of either numerical elastoplastic analysis or shakedown analysis. Elastoplastic analyses (see e.g. Refs. [5, 9, 17, 22, 23]) allow the complete time histories of stress and strain during repeated, cyclic loading to be calculated. However, simulation of realistic load scenarios and problem geometries comes at a very high computational cost. Shakedown analysis, on the other hand, allows the long-term response of a structure subjected to a large number of load cycles to be predicted, without having to compute stresses and strains at a large number of load steps. It is based on two fundamental shakedown theorems, the lower-bound theorem [21] and the upper bound theorem [14], and has been successfully used to in the field of pavement engineering and the design of pavements against excessive rutting (see e.g. Refs. [3, 4, 18, 19, 24, 27, 28, 31, 36, 38]).

The problem of track structure deterioration is similar to that of pavement degradation, however, owing to the complexity of the track structure, numerical techniques are required to obtain the shakedown limit load. The rapid development of computational methods over the last two decades has facilitated a number of numerical shakedown analysis studies relevant to railway engineering (see e.g. Refs. [2, 13, 20, 29, 33, 34, 37]). However, the majority of these studies focused on the rolling contact fatigue between wheels and rails. Less attention has been paid to the performance of the track substructure (ballast, sub-ballast, subgrade), despite the fact that the performance of the components of the substructure under cyclic rail traffic loads can be critical for the cost of track maintenance [30]. For example, Ishikawa et al. [11] provide evidence that track deterioration is predominantly triggered by uneven subsidence of the substructure of the railway.

The overarching aim of this study is to investigate the effect of the performance of the substructure under cyclic loads on the shakedown limit load with numerical methods and obtain reliable estimates of the latter while minimising computational cost. To achieve this aim, three-dimensional (3D) finite element (FE) models of varying degree of complexity are prepared, to quantify the effect of the level of detail of the simulation on the results. In previous studies (see e.g. Refs. [16, 30]) certain simplifying assumptions have been embraced, such as representation of moving train loads as equivalent concentrated loads acting on either the surface of the sleepers or directly on the ballast layer. This suggests that the kinematic interaction between the rails and their support (pads–sleeper–ballast) is not accounted for in the solution. To investigate this, Melan's lower-bound shakedown theorem is employed here to obtain the shakedown load, using elastic stress fields obtained from numerical analyses. Accordingly, two simplified FE models are established, in which the wheel loads are represented as equivalent loads acting either on the surface of the sleepers or on the ballast layer. Results from the simplified FE models are compared against those of the detailed, benchmark 3D model, in terms of elastic stress fields, to quantify the effect of considering kinematic interaction and the level of analysis detail on the practical results, and to optimise the balance between computational cost and accuracy of the solution. Finally, a parametric shakedown analysis of the ballasted track structure is performed, to investigate the effect of problem parameters on the shakedown limit.

2 Outline of the shakedown solution

2.1 Melan' lower-bound shakedown theorem

Melan' lower-bound shakedown theorem is used in this study to find the shakedown limit load [21]. This states that an elastic-perfectly plastic structure will shakedown under repeated or cyclic loads if the yield condition at any point is not violated by a total stress field which comprises the self-equilibrated residual stress field, and the elastic stress field from the external load. If the external load is denoted by λp_0 (p_0 may be conveniently set equal to the unit pressure in the calculations) and λ is the shakedown multiplier (a dimensionless scale parameter), then all the elastic stress components associated with the external load are also proportional to λ. Hence, Melan's shakedown theorem is expressed as:

$$f\left(\lambda\sigma_{ij}^{\mathrm{e}} + \sigma_{ij}^{\mathrm{r}}\right) \leq 0 \tag{1}$$

where $\lambda\sigma_{ij}^{\mathrm{e}}$ is the elastic stress field due to the external pressure λp_0, σ_{ij}^{r} is the residual stress field and $f(\sigma_{ij}) = 0$ is the yield condition for the material. Note that the shakedown load is computed using a numerical elastic stress field, rather than an exact closed form one, so that the solution is best described as a quasi-lower bound.

2.2 Numerical evaluation of the shakedown limit

Residual stresses are what remain in the structure after repeated load applications as a result of plastic deformation. In elastic–plastic structures under cyclic or repeated loads, residual stresses developed during a loading and unloading process may help the structure to resist further yield. This leads to the shakedown phenomenon—the structure finally responds purely elastically to the subsequent load cycles and exhibit no further plastic strains,

which has been comprehensively examined by Hadda and Wan [10] in terms of the mechanics and physics of granular material responses at the macroscopic and microscopic levels during both monotonic and cyclic loadings. Alternatively, the residual stresses developed in the structure may be incapable of preventing continuing plastic strains and finally result in structural failure in such a way of either alternating plasticity or unlimited incremental plasticity. This happens even if the applied load is below the limit determined by limit analysis. According to the Melan's shakedown theorem, the structure is under safe state if there is one residual stress found and the sum of the residual stress and the elastic stress does not violate the yield criterion of materials. Therefore, the calculation of the shakedown limit load is attributed to the determination of the critical residual stress.

For the railway structure under moving train loads, the residual stress field, which is different with that in pavement, may be more complicated owing to the complexity of structural geometry, load distribution and boundary conditions. Calculation of the shakedown limit requires the establishment of a residual stress field in the half-space defined by the plane where external loads are acting, viz. the stresses resulting when the magnitude of the load is sufficient to induce plastic deformations. Here we assume that surface of the half-space remains horizontal, i.e. no uneven subsidence takes place, for the quasi-static situation, the stresses induced in the ground are independent of the longitudinal coordinate (x-coordinate). This means that all points located in one longitudinal alignment will experience the same cyclic stresses with just a time delay. This conclusion is valid if the soil is assumed as homogenous and isotropic. Therefore, in order to obtain a time-independent residual stress field, it will be mandatory independent of the longitudinal direction. For the 3D problem of moving traffic loads, the critical plane is the vertical plane xz defined by the travel direction x and the vertical axis z [36]. The critical nonzero residual stress component in this plane is denoted as σ_{xx}^{r} and is as a function of y and z.

The total stress on any vertical plane xz (y = constant) can be expressed as follows:

$$\begin{aligned}\sigma_{xx} &= \lambda\sigma_{xx}^{\mathrm{e}} + \sigma_{xx}^{\mathrm{r}}\\ \sigma_{zz} &= \lambda\sigma_{zz}^{\mathrm{e}}\\ \sigma_{xz} &= \lambda\sigma_{xz}^{\mathrm{e}}\end{aligned} \tag{2}$$

Assuming that soil/substructure material obeys the Mohr–Coulomb yield criterion, and treating tensile stresses as positive, the requirement to satisfy Melan's shakedown theorem (Eq. 1) leads to the following expression [36, 38]:

$$f = \left(\sigma_{xx}^{\mathrm{r}} + M\right)^2 + N \le 0 \tag{3}$$

where

$$\begin{aligned}M &= \lambda\sigma_{xx}^{\mathrm{e}} - \lambda\sigma_{zz}^{\mathrm{e}} + 2\tan\varphi\left(c - \lambda\sigma_{zz}^{\mathrm{e}}\tan\varphi\right)\\ N &= 4\left(1+\tan^2\varphi\right)\left[\left(\lambda\sigma_{xz}^{\mathrm{e}}\right)^2 - \left(c - \lambda\sigma_{zz}^{\mathrm{e}}\tan\varphi\right)^2\right]\end{aligned} \tag{4}$$

and c is the apparent cohesion and φ is the friction angle of the half-space material. Satisfying the shakedown condition (Eq. 3) requires that:

$$N \le 0 \Rightarrow \lambda \le c/\left|\sigma_{xz}^{\mathrm{e}}\right| + \sigma_{zz}^{\mathrm{e}}\tan\varphi \tag{5}$$

By searching for the maximum value of $\left|\sigma_{xz}^{\mathrm{e}}\right| + \sigma_{zz}^{\mathrm{e}}\tan\varphi_n$ throughout the half-space, we can determine a shakedown limit multiplier, as discussed by Yu [36]. However, this method neglects both the equilibrium and yield constraints on the residual stresses in the calculation of the shakedown limit, and therefore results in an "upper bound type 1" solution, according to the definition of Krabbenhøft et al. [15]. To address this issue, a lower bound on the shakedown limit multiplier, λ_{SD}, can be computed based on the procedures proposed by Zhao et al. [38] and Krabbenhøft et al. [15], which essentially result in identical results to the method of conics proposed by Sharp and Booker [31].

The above is valid for a homogeneous half-space, which of course is not the case for a ballasted track substructure, which comprises several layers of different materials, featuring different mechanical properties. In a multi-layered profile, the shakedown limit multiplier λ_{SD} can be determined through searching the minimum value of the shakedown limits in each individual layer as:

$$\lambda_{\mathrm{SD}} = \min\left(\lambda_{\mathrm{SD}}^1, \lambda_{\mathrm{SD}}^2, \lambda_{\mathrm{SD}}^3, \ldots, \lambda_{\mathrm{SD}}^m\right) \tag{6}$$

where the shakedown limit multiplier λ_{SD}^i of the i-th layer is obtained by modifying Eq. (5) as:

$$\lambda_{\mathrm{SD}}^i = \frac{c_i}{\max\left(\left|\sigma_{xz}^{\mathrm{e}}\right| + \sigma_{zz}^{\mathrm{e}}\tan\varphi_i\right)} \tag{7}$$

and c_i and φ_i are the shear strength parameters of the i-th layer.

The elastic stress field in a layered profile is more complicated compared to that in a homogeneous half-space, and deriving an analytical solution to describe it is particularly cumbersome. Therefore, a closed-form expression for the shakedown limit multiplier will not be sought. Instead, the problem is solved numerically with the implicit version of the Finite Element code ABAQUS. Searching for the shakedown limit multiplier (Eqs. 6, 7) is performed via a custom subroutine UVARM that allows automatically screening for the maximum value of $\left|\sigma_{xz}^{\mathrm{e}}\right| + \sigma_{zz}^{\mathrm{e}}\tan\varphi_i$ at every integration point of the elements of each layer, which is particularly important when dealing with

three-dimensional problem geometries. In this way, the shakedown multiplier for each layer λ_{SD}^{i} is obtained, and the shakedown limit of the track substructure is obtained from Eq. (6). The numerical models used to obtain the shakedown limit with this procedure are described in the following.

3 Finite element models for the track structure

The elastic stresses due to the external load (Eq. 7) are obtained numerically using a full 3D FE model (Model A, see Zhuang and Wang [39]). In addition, two simplified models with reduced computational and preparation costs are utilised. In these models, the rail and railpads are not simulated, and loads are applied directly on the surface of the sleepers (Model B), or on the sub-ballast (Model C).

3.1 Full 3D FE model (Model A)

The FE mesh of Model A is shown in Fig. 1. Since the problem is symmetric, half of the track structure is simulated. The rail (CHN 60 kg/m) is 176 mm high with cross-sectional area 7.745 × 10^5 mm^2 and is modelled with solid elements (C3D8R). The rail rests on discrete railpads, which are modelled as a spring element (SPRINGA), with a vertical stiffness of 150 MN/m [8]. The concrete monoblock sleepers feature dimensions 2.6 m × 0.2 m × 0.2 m (length × width × height) are spaced at 0.65 m. The substructure comprises the ballast, sub-ballast, subgrade and embankment. The total simulated thickness is 6.7 m. The length of the track considered is limited to 15 sleeper bays, considering the computational effort required to solve the 3D problem in the time domain, and the sleepers are assumed to be in perfect contact (no slip) with the ballast along the sleeper length [25]. The vertical boundaries of the track structure are restrained against horizontal movement normal to each face, and a restraint is applied on both the horizontal and vertical movements at the bottom face. The response of the rail and sleepers is assumed to be linear elastic, while the geomaterials comprising the track substructure are modelled with solid C3D8R elements as elastic (when seeking to calculate the elastic stress field) or elastic-perfectly plastic obeying the Mohr–Coulomb failure criterion (when seeking to calculate the shakedown multiplier). The material properties and layer thickness are given in Tables 1, 2, 3, 4.

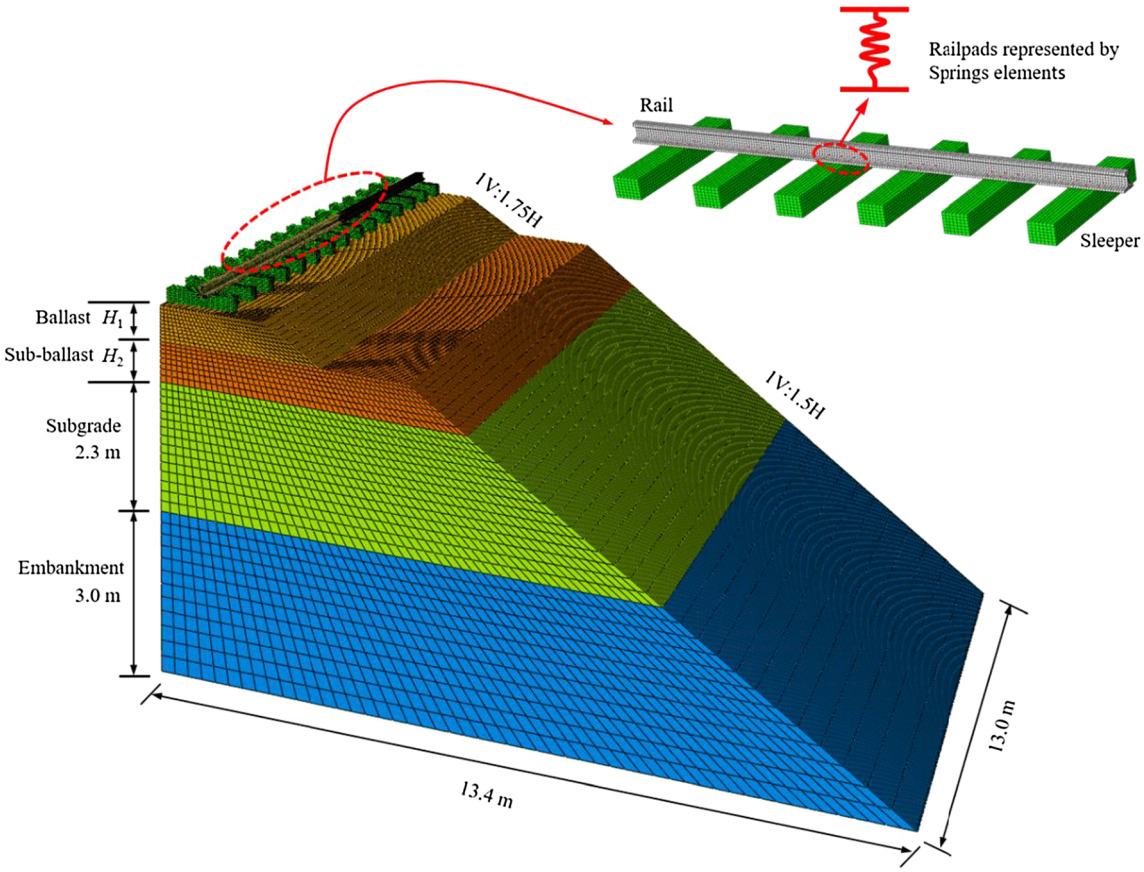

Fig. 1 Finite element model of the ballasted track structure

Table 1 Material properties of the ballasted track structure

Layers	Model	E (MPa)	v	c (kPa)	φ (°)
Rail	Elastic	200,000	0.30	–	–
Sleeper	Elastic	30,000	0.20	–	–
Ballast	Mohr–Coulomb	E_1	0.25	1	φ_1
Sub-ballast	Mohr–Coulomb	E_2	0.25	1	45
Subgrade	Mohr–Coulomb	60	0.25	5	40
Embankment	Mohr–Coulomb	40	0.25	5	35
Railpads	Vertical stiffness k_p = 150 MN/m				

Table 2 Material properties of the ballast and sub-ballast

φ_1 (°)	25	35	**45**	55	65	75
E_1 (MPa)	100	**200**	300	400	500	600
E_2 (MPa)	100	**100**	100	100	100	100
E_1/E_2	1	**2**	3	4	5	10

Bold values indicate the parameters used for the basic model

In Model A, the rolling and sliding contact at the wheel-rail interface is modelled as a 3D Hertz load distribution [12], shown in Fig. 2a. The load P is the total normal force applied along the vertical direction due to the wheel rolling, and Q is the total shear force applied along the travel direction due to rolling friction.

Considering the contact surface of the Hertz load to be circular, with radius a, allows the normal and shear pressure p and q to be calculated as:

$$p = \frac{3P}{2\pi a^3}\left(a^2 - x^2 - y^2\right)^{1/2}$$
$$q = \frac{3Q}{2\pi a^3}\left(a^2 - x^2 - y^2\right)^{1/2} \quad (8)$$

The load distribution results in a maximum compressive pressure $p_0 = 3P/(2\pi a^2)$ at the centre of the loaded area ($x = y = z = 0$). The rolling friction coefficient μ between wheel and rail may be assumed to be constant, with the slip between the wheel and the rail being fully developed, so that the shear force is proportional to the normal force, as:

$$Q = \mu P \quad (9)$$

A fine mesh with the element length of around $0.5a$ is adopted for the rail. The mesh size for the sleepers can be slightly coarser, with the element length of a. For the subsystem of the ballasted track structure, the mesh with the element length of $10a$ is used at the loading region, and a relatively coarse mesh is used for the other region. As a result, a total number of the elements used in each simulation is approximately 405,000. The sensitive to mesh size is checked. When halving the mesh size, the shakedown limits are found to slightly changed, with the difference less than 5%, value which was considered suitably small.

Table 4 Thickness of ballast and sub-ballast layers

h_1 (m)	0	0.14	0.28	0.42	0.56	**0.7**
h_2 (m)	1.4	1.26	1.12	0.98	0.84	**0.7**
h_1/h_2	0	1:9	2:8	3:7	4:6	**5:5**

Bold values indicate the parameters used for the basic model

3.2 FE model with equivalent load acting on the surface of sleeper (Model B)

Three-dimensional numerical simulations facilitate the investigation of an important mechanism of track substructure response to rail loads, viz. the transfer of stresses from the wheel to the substructure via the rail–railpads–sleepers combination. Alternatively, a beam-on-elastic-foundation model can be employed to calculate the distribution of stresses from the wheel to the individual sleepers and the substructure, as depicted in Fig. 2b. The rail acts as a beam and distributes the load of an individual wheel over several sleepers—the one directly beneath the wheel and several sleepers on either side of it [1, 6]. The actual number of sleepers that carry a non-trivial portion of the wheel load, and the actual percentage of the wheel load carried by each sleeper, are functions of the stiffness of the beam (i.e. its section), and of the stiffness of the support. The Chinese Code for design of high-speed railways [6] suggests that the point load from the wheel can be distributed among five sleepers, with the simplified distribution shown in Fig. 2b.

This simplified approach was employed to develop an equivalent FE model (Model B), where the rail and railpads are not simulated explicitly. This simplification results in a reduction of the total number of elements to 386,000. The moving train load is represented by five uniformly stressed

Table 3 Layer thickness of the ballasted track structure

Layers	Rail	Sleeper	Ballast	Sub-ballast	Subgrade	Embankment
Thickness (m)	0.176	0.20	h_1	h_2	2.3	3.0

The sum thickness of the ballast and sub-ballast is 1.4 m, and h_1 and h_2 vary with the ratios, as shown in Table 4

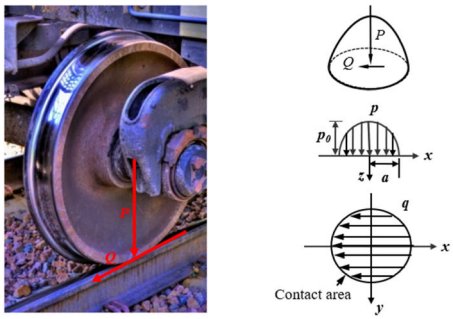

(a) Wheel/rail contact with a 3D Hertz load distribution

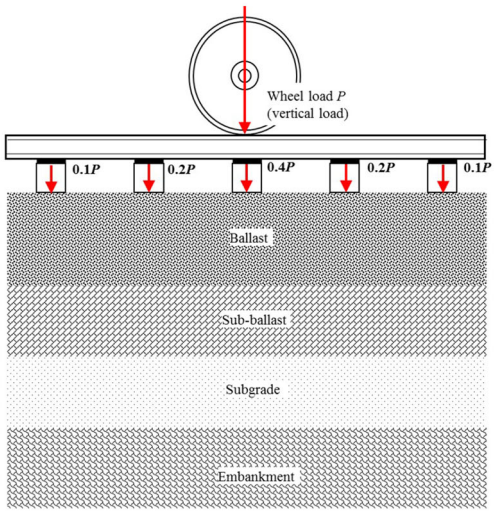

(b) Wheel load distribution on sleepers

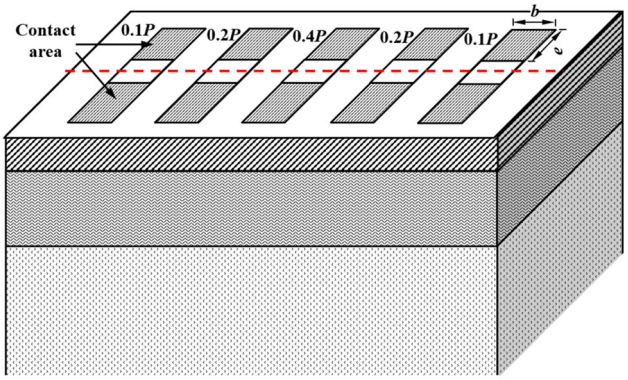

(c) Wheel load distribution on the surface of ballast layer

Fig. 2 Equivalent distribution of wheel load for ballasted track structure

areas, each corresponding to a different sleeper distribution the wheel load, as shown in Fig. 2b. These uniform stress distributions act on the surface of the sleepers, at the area where the rail is in contact with the sleepers. The shear stresses on the surface of sleepers are proportional to the normal stresses and are calculated according to Eq. (9).

3.3 FE model with equivalent load acting on the surface of ballast (Model C)

Model B can be further simplified by omitting the stress redistribution occurring at the sleepers, and assuming that the load from the rail and the railpads is transferred directly to the surface of the ballast. The total number of elements used in the simulation is further reduced to 371,000. The Chinese Code for design of high-speed railways [6] suggests that the wheel load may be uniformly distributed on the surface of the ballast, across an effective bearing area (shaded rectangles in Fig. 2c). The width b of each rectangle comprising the effective bearing area is equal to the width of the sleeper, while e = 1.0 m. Shear stresses acting on the effective bearing area are again proportional to the normal stresses and are calculated according to Eq. (9).

3.4 Comparison of elastic stress fields from the different numerical models

Simplifications introduced in the simulation of rails, railpads and sleepers may reduce the model preparation effort and computational time associated with 3D numerical analyses, but may also affect the accuracy of the elastic stress field, and therefore the estimation of the shakedown limit with the proposed numerical method. This effect can be quantified via a direct comparison of the elastic stress fields calculated with the three FE models viz. Models A, B and C, assuming the Chinese Railways High-speed train (CRH3) with each axle load of 100 kN runs on the ballasted track structure. It is noted that the shakedown analysis is based on a quasi-static assumption, which characterised by the absence of dynamic train-track interaction loads, i.e. this mechanism is due to the passage of the static loads corresponding to the distribution of the static weight of the train by the different wheelsets.

Figures 3, 4, 5 and 6 present the elastic stress field calculated via the three FE models on the surface of ballast and sub-ballast (Figs. 3, 4, 5), and along the thickness of the model (Fig. 6). As discussed above (see Eq. 7), the elastic stress components that govern the shakedown of the track structure are the shear stress σ_{xz} and the vertical normal stress σ_{zz}. Moreover, the critical point for the shakedown lies on one of the vertical xz plane, implying that the stress distribution in the transverse direction may directly affect the shakedown limit of the ballasted track structure. Therefore, the elastic stresses σ_{xz} and σ_{zz} are presented along the direction of travel (x-direction), transverse direction (y-direction) and the thickness of the model (z-direction), along a plane aligned with the wheel (y = constant). The equivalent von Mises (or deviatoric)

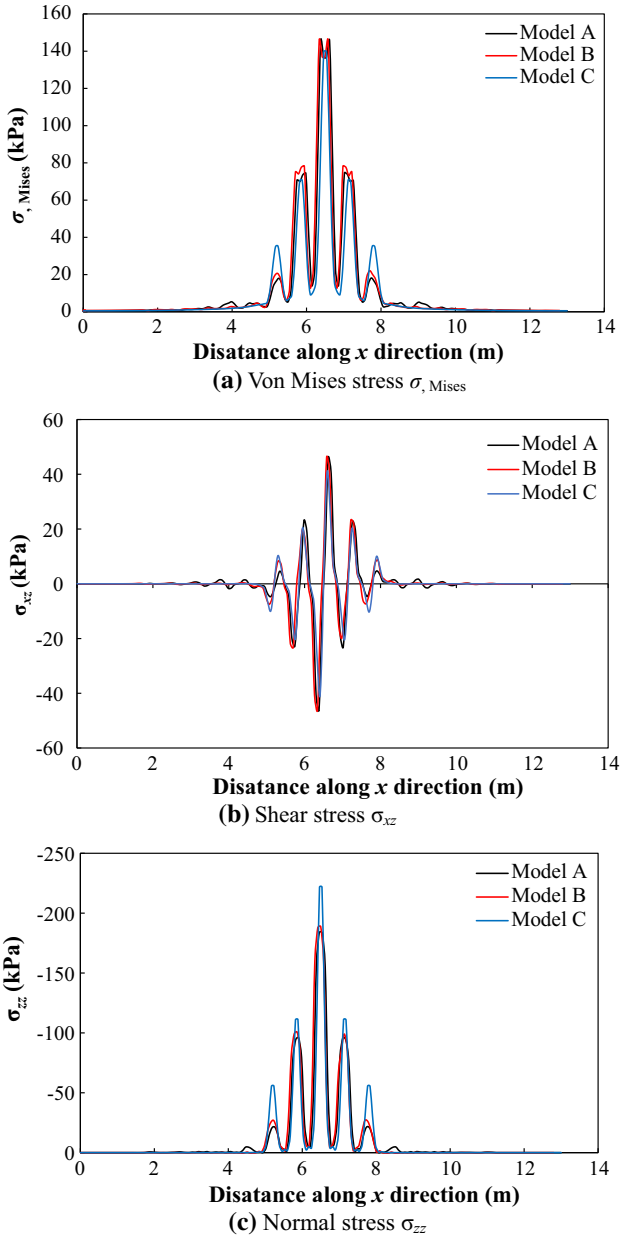

Fig. 3 Elastic stresses on the surface of ballast layer due to wheel loads along the travel (x) direction

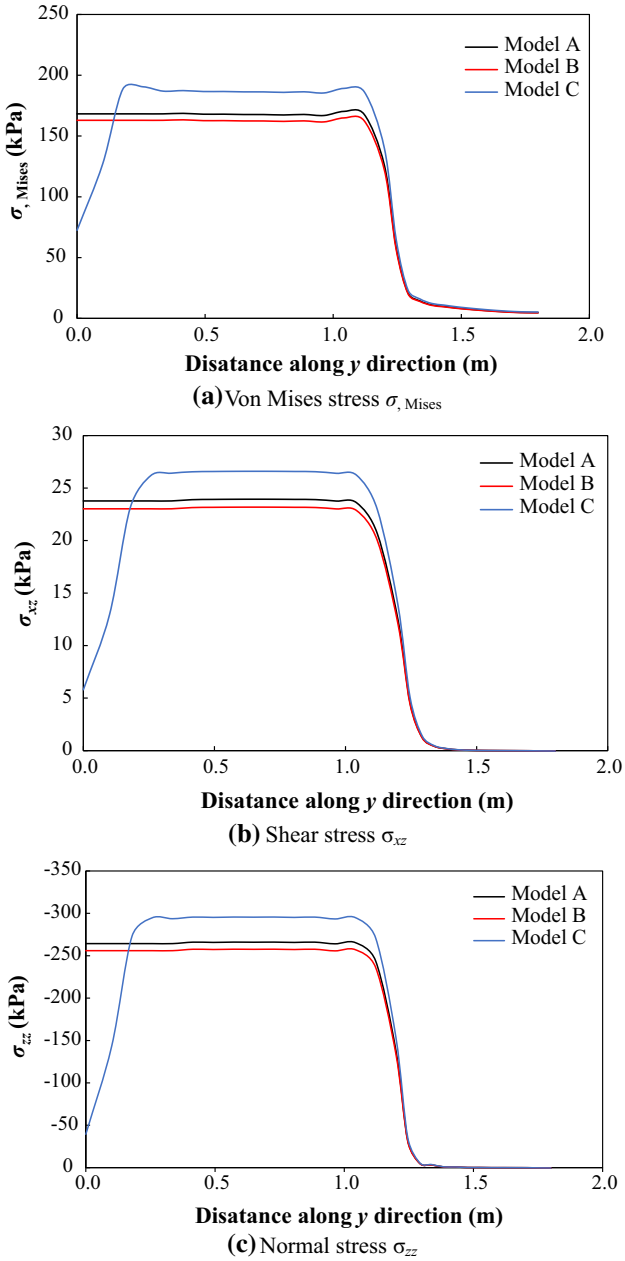

Fig. 4 Elastic stresses on the surface of ballast layer due to wheel loads along the transverse (y) direction

stress σ_{Mises}, which is commonly used in failure criteria, is also included in the comparison.

The stress distributions plotted in Figs. 3, 4 and 5 suggest that the three FE models provide similar elastic stress profiles, and are compatible with the stress distributions presented by Eason [7] and Wei et al. [35]. There are, however, differences in the magnitude of the predicted stresses. As expected, Model B provides stresses which are closer to the benchmark Model A, with the maximum divergence being of the order of 5%. On the other hand, Model C appears to overestimate the normal σ_{zz} stresses on the ballast, and underestimate the normal, shear, and deviatoric stresses in the sub-ballast and the subgrade. This is attributed to the fact that redistribution of stresses by the sleepers is ignored in Model C, as shown in Fig. 4. The maximum divergence between the peak stresses calculated with Model C and Model A is of the order of 25%.

Also observed is that the computation time of Model A is 4.5 h, while that of Model B and Model C reduces by approximately 13% and 19% for the same computer, respectively. This comparison suggests that the simplified Model B is capable of capturing the elastic stress field with acceptable accuracy, compared to the detailed 3D model

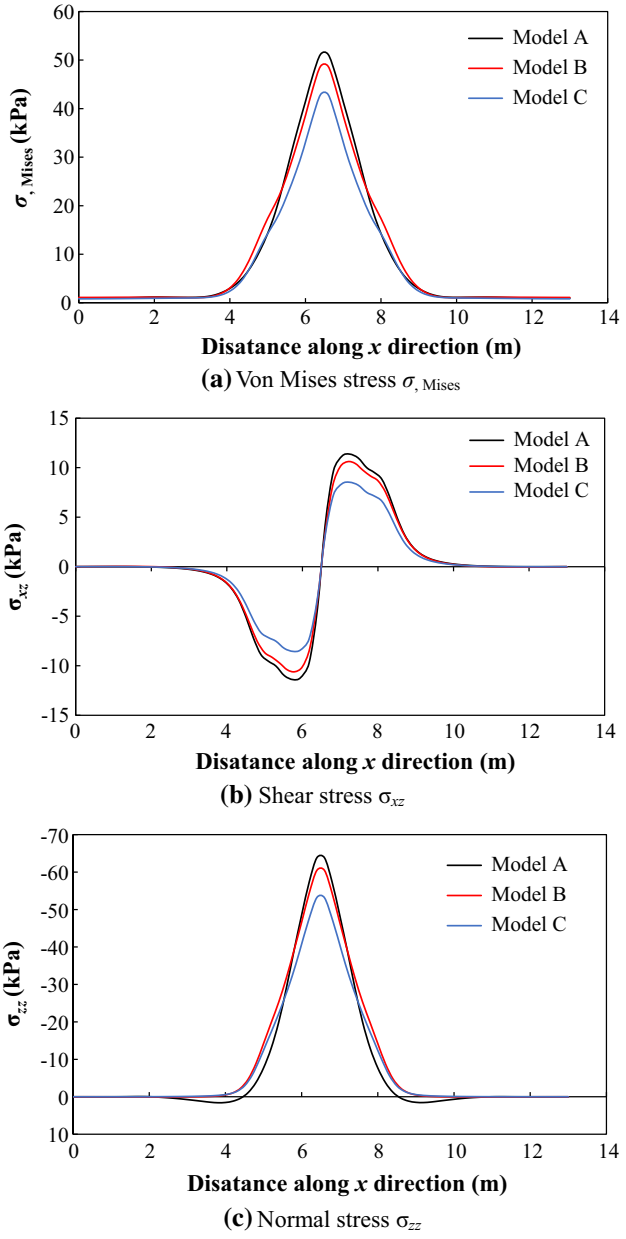

Fig. 5 Elastic stresses on the surface of sub-ballast layer due to wheel loads along the travel (x) direction

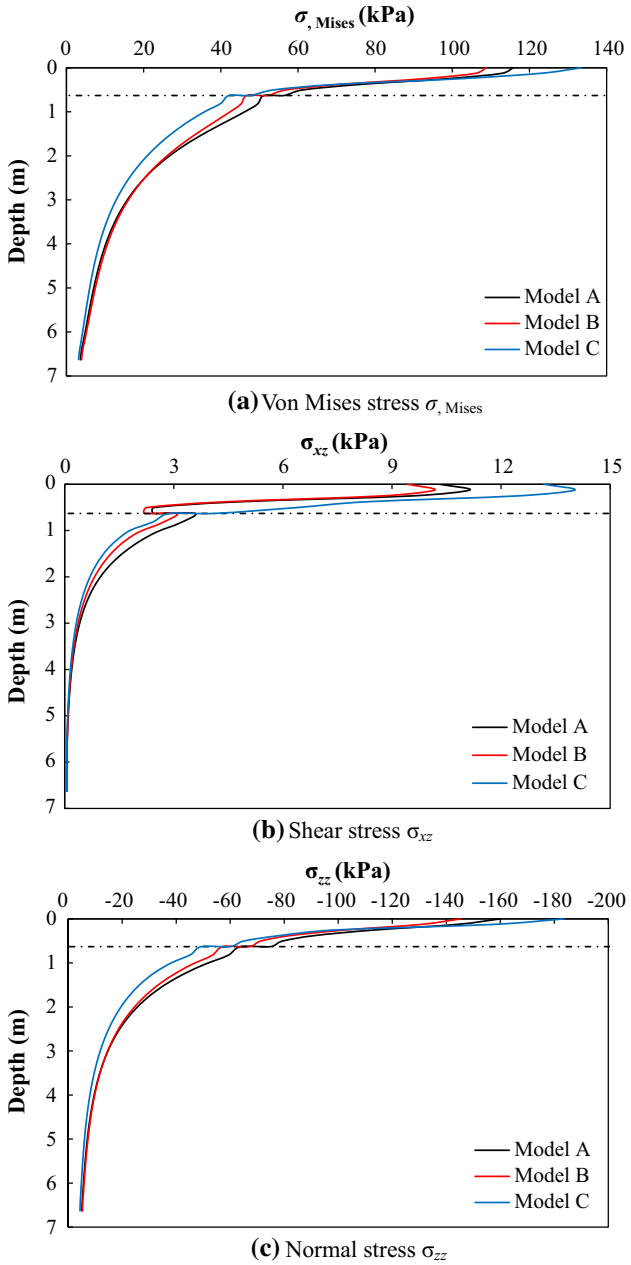

Fig. 6 Elastic stresses due to wheel loads along the thickness of the model

(Model A), at a lower computational cost and less model preparation time. Its use is therefore recommended for the shakedown analysis of a ballasted track structure, and it is adopted for the parametric study presented in the following.

4 Parametric shakedown analysis of ballasted track structure

For the parametric shakedown analysis, the geomaterials in Model B (ballast, sub-ballast, subgrade, embankment) are analysed with the elastic built-in material model in ABAQUS, while failure is introduced via the subroutine UVARM, using the shear strength parameters listed in Table 1. The shakedown limit is found as function of the rolling friction coefficient μ, assumed to vary between a wide range $\mu = 0.0$ and $\mu = 0.5$ in order to explore the sensitivity of results to friction. Other parameters varied during the analyses are the material friction angle φ, the ballast/sub-ballast stiffness ratio E_1/E_2, and the thickness ratio h_1/h_2 (see Tables 2, 3, 4). Note that the sub-ballast parameters are kept constant, so that the parameters of the ballast are modified accordingly to attain the desired

stiffness and thickness ratios. The shakedown limit multiplier determined by Eq. (7) is provided in terms of the normalised shakedown limit $\lambda_{SD}p_{max}/c_1$, where p_{max} is the maximum vertical stress acting on the surface of the sleepers in Model B, and c_1 is the apparent cohesion of ballast.

Figure 7a shows the influence of the ballast/sub-ballast stiffness ratio E_1/E_2 on the normalised shakedown limit defined above, for various rolling friction coefficients. Observe that the normalised shakedown limit decreases considerably with increasing rolling friction, due to the increase in the applied shear force (Eq. 9). Most importantly, there appear to be an "optimum" stiffness ratio E_1/E_2, for which the normalised shakedown limit attains its maximum value. This optimum value, depicted with a red dotted line in Fig. 7a, appears to be independent of the rolling friction coefficient μ. This peak in the normalised shakedown limit corresponds to the maximum resistance of the system and indicates the transition of the critical point for shakedown from the sub-ballast layer to the ballast layer. For a stiffness ratio $E_1/E_2 > 2$, failure always occurs in the ballast layer, and therefore the shakedown limit keeps decreasing with increasing E_1/E_2 values. This can be explained if we take into account the fact that lower stresses propagate to the sub-ballast layer as E_1/E_2 increases, therefore material failure occurs at the base of the ballast layer as the strength parameters of the ballast and sub-ballast are assumed equal in this set of analyses. As the rolling friction coefficient increases the existence of this optimum stiffness ratio becomes less and less important, due to the increased contribution of the shear force whose value does not depend on the stiffness of the system. Still, for realistic μ values, the differences are non-trivial.

The combined effect of the friction angle of the ballast φ_1 and the rolling friction coefficient μ on the normalised shakedown limit is depicted in Fig. 7b. As expected, the material friction angle has a significant effect on the normalised shakedown limit. There appears again to exist an "optimum" shear resistance of the ballast, that provides the maximum resistance of the system to failure, and indicates the transition of the optimum point from the surface to the bottom of the ballast layer, as the shear strength of the former increases. Interestingly, φ_1 values higher than the "optimum" friction angle of the ballast result in a decrease in the maximum resistance to failure. This is attributed to the fact that tensile stresses σ_{zz} develop at the bottom of the ballast layer in the elastic numerical analysis, therefore the factor $\sigma^{c}_{zz}\tan\varphi_i$ in Eq. (7) becomes positive (tensile stresses are taken as positive). When the friction angle is relatively low, the critical point for shakedown is at the surface of the ballast layer. However, when the friction angle increases the critical point is found at the bottom of the ballast layer. There, as $\tan\varphi_i$ increases the denominator in Eq. (7) increases, resulting in lower λ_{SD} values. Furthermore, the normalised shakedown limit is again very sensitive to the value assigned to the rolling friction coefficient. The sensitivity of the normalised shakedown limit to the friction angle of the ballast decreases considerably for high rolling friction coefficient values.

Finally, Fig. 7c presents the effect of the ballast/sub-ballast thickness ratio h_1/h_2 on the normalised shakedown limit, for various rolling friction coefficient values. Note that the total thickness of ballast and sub-ballast is fixed to $h_1 + h_2 = 1.4$ m, while the variation of the individual layer thicknesses with the thickness ratio is listed in Table 4. The results plotted in Fig. 7c confirm that the normalised shakedown limit increases with the relative thickness of the ballast (increasing ballast/sub-ballast ratio h_1/h_2). The normalised shakedown limit reaches an asymptote when the critical point moves from the top of the sub-ballast layer to the ballast layer. This transition point, corresponding to the optimum thickness ratio h_1/h_2, is depicted in Fig. 7c with a dotted red line. As soon as we exceed the optimum ratio, any further increase in the thickness of the ballast will have a trivial effect on the capacity of the track structure viz. the normalised shakedown limit will depend entirely on the material properties of the ballast layer.

5 Concluding remarks

Owing to the complex geometry of the problem, particularly the fact that multiple materials must be considered simultaneously, the shakedown load of a ballasted track structure subjected to moving train loads can be found only with three-dimensional numerical methods. In this study, we investigate how much the simplifications introduced in the geometry of the problem affect the error introduced in determining the quasi-lower bound of the shakedown load with finite elements. The latter was computed from a user-defined subroutine implemented in the code ABAQUS, which provides the shakedown load multiplier from a numerical three-dimensional elastic stress field while exploiting Melan's lower-bound shakedown theorem. The main aim of the comparison presented was to determine the degree of sophistication in the model that results in the optimum balance between accuracy and preparation/analysis cost.

The establishment of a finite element setup that provides accurate estimates of the shakedown load multiplier at reasonable computational cost allowed a parametric study to be performed on the effect of the relative elastic stiffness, thickness and shear strength of the ballast/sub-ballast layers on the maximum capacity of the system. The effect of the relative magnitude of the shear force acting on the

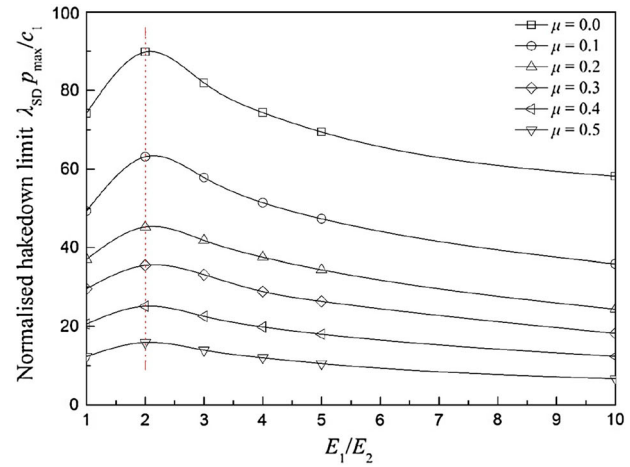

(a) Effect of ballast/sub-ballast stiffness ratio

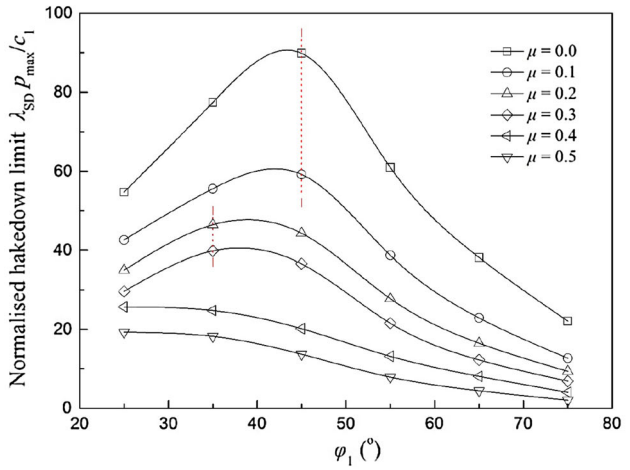

(b) Effect of friction angle of ballast layer

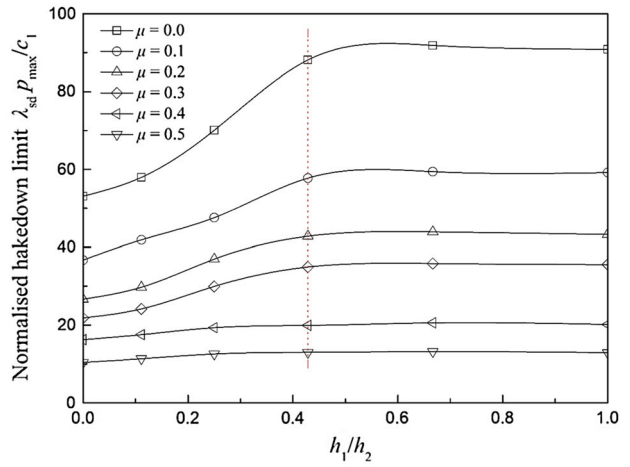

(c) Effect of ballast/sub-ballast thickness ratio

Fig. 7 Results of parametric study on normalised shakedown limit of ballasted track structure

wheel-rail interface was introduced in the parametric study by considering different values of the rolling friction coefficient. Conclusions from this parametric study provide insights on optimising the design of ballasted track against repeated train loads. It should be noted that since the quasi-static train load was applied in the numerical analyses, the dynamic effect due to the dynamic excitation of the train masses during its movement was not considered, which may make the conclusions in this paper to be in the un-conservative side.

Acknowledgements The financial support of National Key R&D Program of China (No. 2016YFC0800200), the financial support sponsored by Qing Lan Project, A Project Funded by the Priority Academic Program Development of Jiangsu Higher Education Institutions (Grant No. 1105007138), the Open Fund of National Engineering Laboratory of Highway Maintenance Technology (No. kfj180106, Changsha University of Science and Technology), and the Fundamental Research Funds for the Central Universities (Grant No. 2242018K40133) is acknowledged. The first author would like to acknowledge the support from China Scholarship Council and the support provided to him by the ARC Centre of Excellence for Geotechnical Science and Engineering at The University of Newcastle, NSW Australia.

References

1. American Railway Engineering and Maintenance-of-Way Association (2012) AREMA manual for railway engineering, vol 1. American Railway Engineering and Maintenance-of-Way Association, Landover
2. Bocciarelli M, Cocchetti G, Maie G (2004) Shakedown analysis of train wheels by Fourier series and nonlinear programming. Eng Struct 26:455–470
3. Boulbibane M, Weichert D (1997) Application of shakedown theory to soils with non-associated flow rules. Mech Res Commun 24(5):516–519
4. Brown SF, Yu HS, Juspi S, Wang J (2012) Validation experiments for lower-bound shakedown theory applied to layered pavement systems. Géotechnique 62(10):923–932
5. Chazallon C, Allou F, Hornych P, Mouhoubi S (2009) Finite elements modelling of the long-term behaviour of a full-scale flexible pavement with the shakedown theory. Int J Numer Anal Meth Geomech 33(1):45–70
6. China Railway Ministry (2010) Code for design of high-speed railway (for trial implementation). China Railway Publishing House, Beijing
7. Eason G (1965) The stresses produced in a semi-infinite solid by a moving surface force. Int J Eng Sci 2(6):581–609
8. Galvin P, Romero A, Dominguez J (2010) Fully three-dimensional analysis of high-speed train–track–soil-structure dynamic interaction. J Sound Vib 329:5147–5163
9. Ghadimi B, Nikraz H, Rosano M (2016) Dynamic simulation of a flexible pavement layers considering shakedown effects and soil-asphalt interaction. Transp Geotech 7:40–58
10. Hadda N, Wan R (2018) Micromechanical analysis of cyclic and asymptotic behaviors of a granular backfill. Acta Geotech. https://doi.org/10.1007/s11440-018-0733-7
11. Ishikawa T, Sekine E, Miura S (2011) Cyclic deformation of granular material subjected to moving-wheel loads. Can Geotech J 48(5):691–703
12. Johnson KL (1985) Contact mechanics. Cambridge University Press, Cambridge

13. Kapoor A, Williams JA (1996) Shakedown limits in rolling-sliding point contacts on an anisotropic half-space. Wear 191(1):256–260
14. Koiter WT (1960) General theorems for elastic–plastic solids. In: Sneddon IN, Hill R (eds) Progress in solid mechanics. North Holland, Amsterdam, pp 165–221
15. Krabbenhøft K, Lyamin AV, Sloan SW (2007) Shakedown of a cohesive-frictional half-space subjected to rolling and sliding contact. Int J Solids Struct 44(11–12):3998–4008
16. Krylov VV, Ferguson C (1994) Calculations of low-frequency ground vibrations from railway trains. Appl Acoust 42:199–213
17. Langueh AMG, Brunel JF, Charkaluk E, Dufrénoy P, Tritsch JB, Demilly F (2013) Effects of sliding on rolling contact fatigue of railway wheels. Fatigue Fract Eng Mater Struct 36(6):515–525
18. Li HX (2010) Kinematic shakedown analysis under a general yield condition with non-associated plastic flow. Int J Mech Sci 52:1–12
19. Li HX, Yu HS (2006) A nonlinear programming approach to kinematic shakedown analysis of frictional materials. Int J Solids Struct 43:6594–6614
20. Makino T, Kato T, Hirakawa K (2012) The effect of slip ratio on the rolling contact fatigue property of railway wheel steel. Int J Fatigue 36(1):68–79
21. Melan E (1938) Theorie Statisch Unbestimmter Tragwerke aus idealplastischem Baustoff. Sitzungsbericht der Akademie der Wissenschaften (Wien) Abt IIA 195:145–195
22. Naeimi M, Li Z, Petrov R, Dollevoet R, Sietsma J, Wu J (2014) Substantial fatigue similarity of a new small-scale test rig to actual wheel-rail system. World Acad Sci Eng Technol 8:1830–1838
23. Nejad RM, Farhangdoost K, Shariati M (2015) Numerical study on fatigue crack growth in railway wheels under the influence of residual stresses. Eng Fail Anal 52:75–89
24. Nguyen AD, Hachemi A, Weichert D (2008) Application of the interior-point method to shakedown analysis of pavements. Int J Numer Meth Eng 75(4):414–439
25. Nguyen K, Goicolea JM, Galbadon F (2014) Comparison of dynamic effects of high-speed traffic load on ballasted track using a simplified two-dimensional and full three-dimensional model. Proc Inst Mech Eng F J Rail Rapid Transit 228(2):128–142
26. Paixão A, Fortunato E, Calçada R (2015) The effect of differential settlements on the dynamic response of the train-track system: a numerical study. Eng Struct 88:216–224
27. Raad L, Weichert D (1995) Stability of pavement structures under long term repeated loading. In: Mroz Z, Weichert D, Dorosz S (eds) Inelastic behaviour of structures under variables loads. Kluwer Academic Publishers, Dordrecht, pp 473–496
28. Raad L, Weichert D, Najm W (1988) Stability of multilayer systems under repeated loads. Transp Res Rec 1207:181–186
29. Ringsberg JW, Franklin FJ, Josefson BL, Kapoor A, Nielsen JC (2005) Fatigue evaluation of surface coated railway rails using shakedown theory, finite element calculations, and lab and field trials. Int J Fatigue 27(6):680–694
30. Selig ET, Waters JM (1994) Track geotechnology and substructure management. Thomas Telford, London
31. Sharp RW, Booker JR (1984) Shakedown of pavements under moving surface loads. J Transp Eng 110(1):1–14
32. Suiker AS, de Borst R (2003) A numerical model for the cyclic deterioration of railway tracks. Int J Numer Meth Eng 57(4):441–470
33. Taraf M, Zahaf EH, Oussouaddi O, Zeghloul A (2010) Numerical analysis for predicting the rolling contact fatigue crack initiation in a railway wheel steel. Tribol Int 43:585–593
34. Van KD, Maitournam MH (2003) Rolling contact in railways: modelling, simulation and damage prediction. Fatigue Fract Eng Mater Struct 26(10):939–948
35. Wei X, Wang G, Wu R (2016) Prediction of traffic loading-induced settlement of low-embankment road on soft subsoil. Int J Geomech 17(2):06016016
36. Yu HS (2005) Three-dimensional analytical solutions for shakedown of cohesive-frictional materials under moving surface loads. Proc R Soc A Math Phys Eng Sci 461:1951–1964
37. Zhao X, Li Z (2015) A three-dimensional finite element solution of frictional wheel–rail rolling contact in elasto-plasticity. Proc Inst Mech Eng J J Eng Tribol 229(1):86–100
38. Zhao J, Sloan SW, Lyamin AV, Krabbenhøft K (2008) Bounds for shakedown of cohesive-frictional materials under moving surface loads. Int J Solids Struct 45(11):3290–3312
39. Zhuang Y, Wang KY (2017) Three-dimensional shakedown analysis of ballasted railway structures under moving surface loads with different load distributions. Soil Dyn Earthq Eng 100:296–300